Electronic Supplementary Material (ESI) for Dalton Transactions.
This journal is © The Royal Society of Chemistry 2021

Supplementary Information for

Constructing high-performance $H_3PW_{12}O_{40}/CoS_2$ CEs of QDSSCs by reducing the surface work function of CoS_2

Tingting Zhang, Qiu Zhang, Yumeng Wang, Fengyan Li,* Lin Xu*

Key Laboratory of Polyoxometalate Science of Ministry of Education, Department of Chemistry, Northeast Normal University, Changchun, Jilin 130024, P. R. China

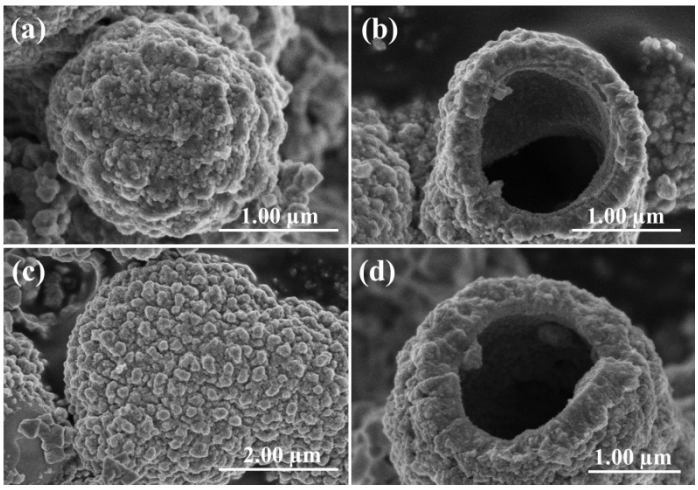

Fig. S1 The morphology of PW_{12}-1/CoS_2 (a,b); the morphology of PW_{12}-3/CoS_2 (c,d).

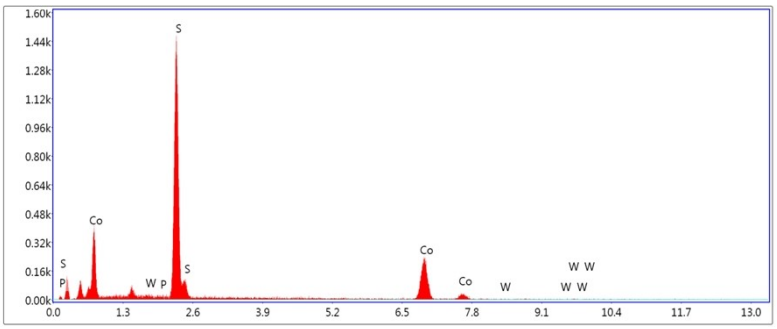

Fig. S2 EDX diagram of PW_{12}-2/CoS_2 complex.

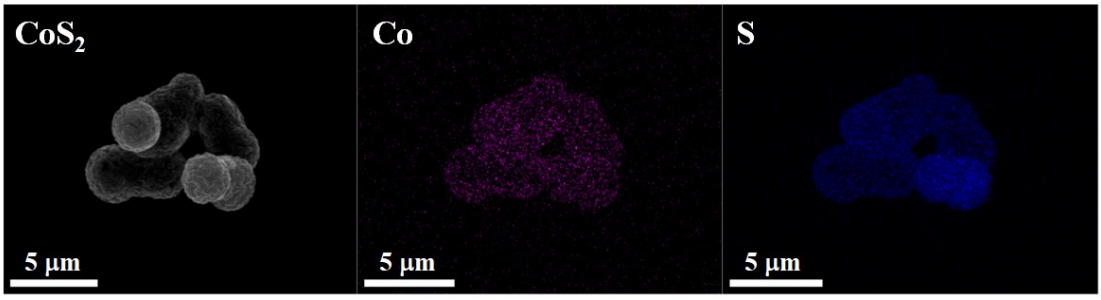

Fig. S3 EDX elemental mappings Co and S inCoS_2.

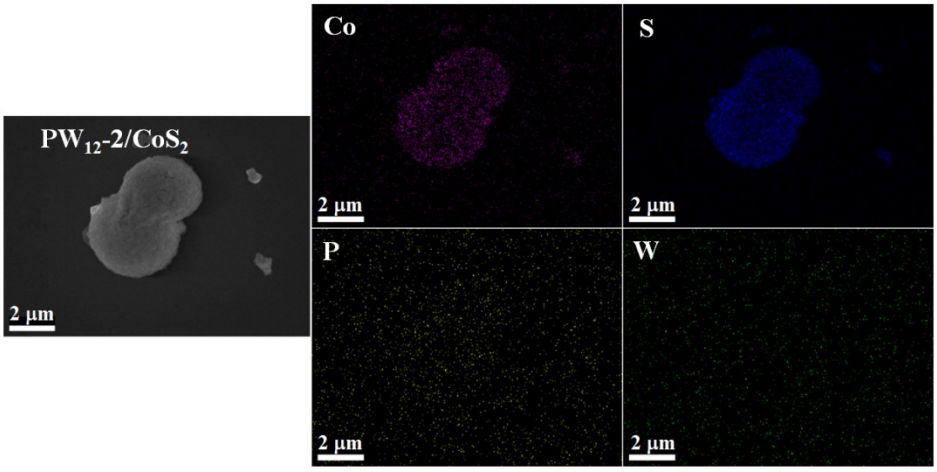

Fig. S4 EDX elemental mappings Co, S, P and W in PW_{12}-2/CoS_2 complex.

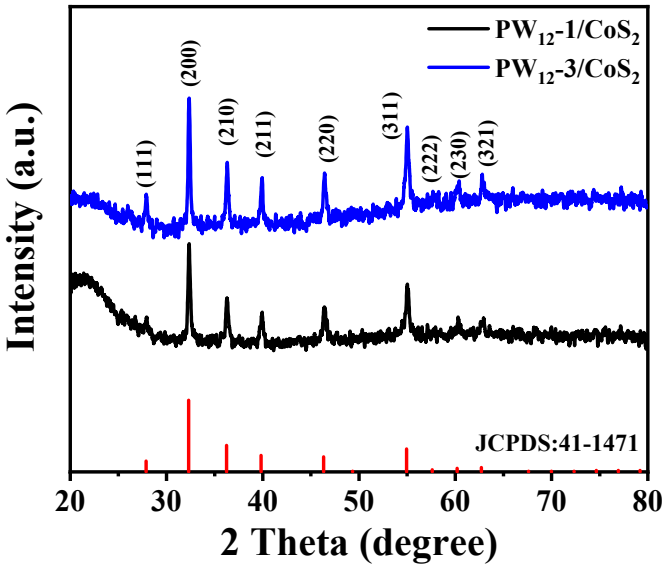

Fig. S5 XRD patterns of the PW_{12}-1/CoS_2 and PW_{12}-3/CoS_2.

PW_{12}-1/CoS_2 and PW_{12}-3/CoS_2 complexs have obvious diffraction peaks at 2 θ =27.9°, 32.2°, 36.4°, 39.7°, 46.4°, 54.9°, 57.6°, 60.2° and 62.6°, which correspond to (111), (200), (210), (211), (220), (311), (222), (230) and (321) crystal surfaces of cubic CoS_2, and are similar to CoS_2. Since the content of PW_{12} in the PW_{12}/CoS_2 is relatively low, no characteristic diffraction peak of PW_{12} has been detected.

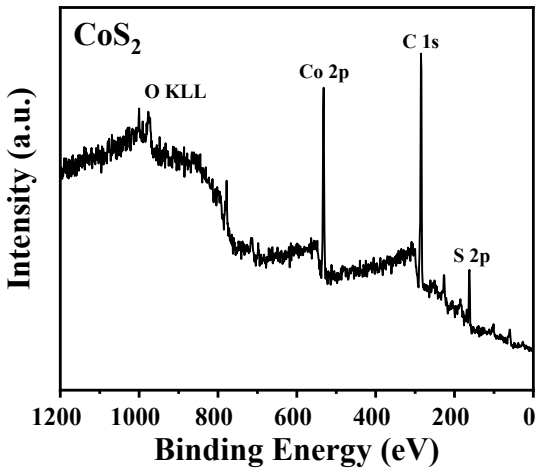

Fig. S6 XPS survey scan spectrum of the CoS_2.

Table S1 Photovotaic parameters of ten QDSSCs based on both CoS_2 and PW_{12}-2/CoS_2 CEs.

cells	J_{sc} [mA cm^{-2}]	V_{oc} [V]	FF	PCE [%]
	16.67	0.453	0.37	2.81
	19.28	0.551	0.32	3.41
	17.15	0.468	0.39	3.89
	16.58	0.585	0.40	3.92
CoS_2	17.17	0.568	0.38	3.75
	19.08	0.575	0.36	3.94
	18.08	0.589	0.35	3.73
	16.67	0.560	0.35	3.25
	16.58	0.576	0.32	3.50
	17.67	0.583	0.36	3.74
	23.42	0.640	0.43	6.33
	22.75	0.651	0.42	6.28
	22.33	0.667	0.43	6.41
	21.99	0.655	0.42	6.05
PW_{12}-2/CoS_2	21.05	0.662	0.45	6.29
	20.94	0.653	0.42	5.75
	22.24	0.660	0.43	6.31
	20.12	0.611	0.43	5.28
	22.02	0.648	0.44	6.28
	20.82	0.595	0.41	5.08

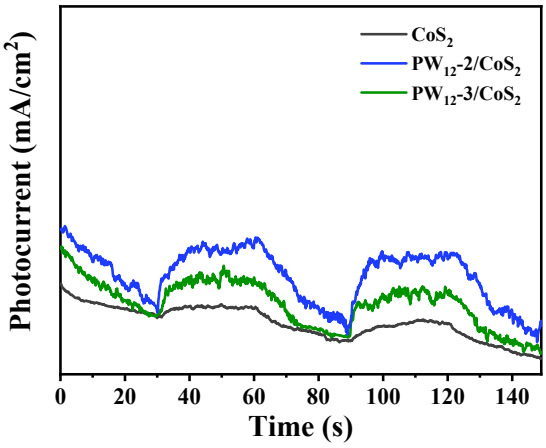

Fig. S7 Transient photocurrent response of CoS_2、PW_{12}-2/ $CoS_2$and PW_{12}-3/ CoS_2.

The test result (Figure S7) showed that the photocurrent response of PW_{12}-3/ CoS_2 decreased compared with PW_{12}-2/ CoS_2, indicating that the doping amount of PW_{12} in CoS_2 increased, the separation of photoelectric carriers and electron mobility both showed a trend of decline, thus leading to the weakening of photovoltaic performance.

Table S2. Result comparisons of present performance parameters with other reports of the same CdS/CdSe QDs co-sensitized photoanode.

Counter electrode	QD	Jsc (mA/cm^2)	Voc (V)	FF	PCE (%)	Reference
PW_{12}-2/CoS_2	CdS/CdSe	21.05	0.662	0.45	6.29	Present work
Cu_2S	CdS/CdSe	19.7	0.544	0.437	4.68	1
CuS	CdS/CdSe	13.36	0.57	0.52	3.95	2
MoS_2-CuS	CdS/CdSe	21	0.48	0.481	5	3
$PMnCoS_4$/CNTs	CdS/CdSe	18.45	0.58	0.45	4.85	4
PbSe	CdS/CdSe	16.91	0.57	0.48	4.67	5
CoO	CdS/CdSe	20.42	0.655	0.45	6.02	6
Tdi_3C_2/CuS	CdS/CdSe	20.86	0.56	0.45	5.11	7
Cu_xS/C	CdS/CdSe	16.96	0.584	0.567	5.62	8
$Cu_{2-x}Se$	CdS/CdSe	21.39	0.567	0.586	7.11	9
GO/(Cu-Co)	CdS/CdSe	24.1	0.68	0.53	8.73	10

[1] C. K. Kamaja, R. R. Devarapalli, Y. Dave, J. Debgupta, M. V. Shelke. *J. Power Sourceces*, 2016, **315**, 277-283.
[2] D. Liu, J. Liu, J. Liu, S. Liu, C. Wang, Z. Ge, X. Hao, N. Du, H. Xiao. *J. Mater.*

Sci., 2019, **54**, 4884-4892.
[3] C. K. Kamaja, R. R. Devarapalli, M. V. Shelke. *ChemElectroChem*, 2017, **4**, 1984–1989.
[4] W. Li, L. He, J. Zhang, B. Li, Q. Chen, Q. Zhong. *J. Phys. Chem. C*, 2019, **123**, 21866-21873.
[5] B. B. Jin, Y. F. Wang, X. Q. Wang, J. H. Zeng. *Appl. Surf. Sci.*, 2016, **369**, 436–442.
[6] Q. Zhang, Z. Jin, F. Li, Z. Xia, Y. Yang, L. Xu. *Sol. Energ. Mat. Sol. C.*, 2019, **206**, 110307.
[7] Z. Tian, Z. Qi, Y. Yang, H. Yan, Q. Chen, Q. Zhong. *Inorg. Chem. Front.*, 2020, 7, 1-9.
[8] I. P. Liu, H. Teng, Y. L. Lee. *J. Mater. Chem. A*, 2017, **5**, 23146–23157.
[9] Y. Bai, C. Han, X. Chen, H. Yu, X. Zong, Z. Li, L. Wang. *Nano Energy*, 2015, **13**, 609–619.
[10] L. Givalou, D. Tsichlis, F. Zhang, C. S. Karagianni, M. Terrones, K. Kordatos, P. Falaras. *Catal. Today*, 2020, **355**, 860-869.